International Journal of Thermal Technologies
ISSN 2277 - 4114

Available at http://inpressco.com/category/ijtt

Research Article

Dryout Characteristics of R134a in a Vertical Minichannel

Zahid Anwar[a*]

[a]Mechanical Engineering Department, University of Engineering and Technology Lahore, KSK Campus, Pakistan

Accepted 24 May 2013, Available online 1June 2013, **Vol.3, No.2 (June 2013)**

Abstract

From safety and efficiency point of view all practical devices should be operated below their associated critical limits. Deteriorated heat transfer alongwith burnout of the test section is the major penalty for moving beyond these limits. This article reports experimental finding on dryout of R134a in a resistively heated, smooth vertical stainless steel minichannel (1.6mm inside diameter and 245 mm heated length). Experiments were conducted at 27 & 32 ^{o}C saturation temperature with 100-500 kg/m^{2}s mass flux and till dryout conditions. Results for mass flux, vapor quality and system pressure are discussed in detail. Experimental findings were compared with various macro and micro scale correlations from the literature, this comparison revealed Wu's correlation (Z. Wu et al, 2011) as the most accurate one for predicting dryout heat flux for R134a in small channels.

Key words: *Correlation, Dryout, Minichannel, R134a*

Introduction

Boiling is the obvious choice for transferring high heating/cooling loads over small temperature lifts. As per Kandlikaar (S. Kandlikar et al, 2006), channels having hydraulic diameter within 200µm-3mm range are considered as minichannels. Compactness in size offer many potential benefits like, enhanced heat transfer (increased surface area), less fluid inventory, less material cost etc.

Critical heat flux refers to the specific operating condition when heater surface is totally blanketed with vapor, this result in sharp increase of heater surface temperature and eventually burnout in heat flux controlled applications. This normally happens close to the outlet of the test section with deteriorated heat transfer due to poor thermal conductivity of vapor compared with the liquid.

Ong (C. L. Ong et al 2011) conducted CHF experiments for R134a, R236fa and R245fa in horizontal small tubes (1.03, 2.2 and 3.04 mm inside diameter). They observed that the CHF increased with reducing diameter until a certain threshold value (0.79 mm in that case) and then decreases with further shrinking the tube size, furthermore CHF increased with increasing mass velocity and decreased with increasing saturation temperature however no influence of subcooling was observed. They proposed a new correlation for predicting CHF, this is a modified version of Wojtan's (L. Wojtan et al, 2006) correlation and includes channel confinement and viscous interfacial shear effects.

Mikielewicz (D. Mikielewicz et al, 2013) reported experimental findings on dryout for four mediums (SES 36, R134a, R123 & ethanol) in small, vertical, silver tubes (1.15 and 2.3 mm in diameter) with 40-900 kg/m^{2}s mass velocities. They observed that dryout heat flux increased with increasing mass flux, with the decrease of vapor quality and with the increase in tube diameter. They also suggested a correlation for prediction of dryout heat flux based on their experimental database.

Callizo (C. M. Callizo et al, 2010) conducted experimental study on critical heat flux with R134a, R22 and R245fa in a 640 µm vertical circular channel (185-335 kg/m^{2}s at saturation temperature of 30 and 35 ^{o}C). Experimental findings revealed that dryout heat flux increased with increasing mass flux however no significant effect of varying saturation temperature was there. Based on their experimental data they proposed a correlation for prediction of critical heat flux, this was a modified version of Wojtan's (L. Wojtan at al, 2006) correlation and gave good predictions as confirmed by other authors like (M. H. Maqbool et al, 2012).

Ali (R. Ali et al, 2011) conducted dryout tests for R134a in vertical, single stainless steel tubes (1.22 and 1.7 mm inside diameter and 220 mm heated length) at two operating pressures corresponding to 27 and 32 ^{o}C saturation temperatures, other operating parameters were mass flux 50-600 kg/m^{2}s. They noticed that dryout heat flux increased with increasing mass flux, decreased with reducing tube diameter while remains unchanged with varying operating pressure.

Maqbool (M. H. Maqbool et al, 2012) conducted dryout experiments with propane in resistively heated

*Corresponding author: Zahid Anwar

vertical tubes (1.7 and 1.224 mm inside diameter 245 mm heated length) with 100-500 kg/m^{2}s mass flux and at three saturation temperatures (23, 33 & 43 ^{o}C). They observed similar parametric effects like Ali (R. Ali et al, 2012) (both used the same experimental setup).

From safety and efficiency point of view, safe operational range must clearly be identified. This experimental study is therefore conducted with R134a in a single vertical channel; experimental results are compared with various correlations (macro and micro scale) from the literature to see their prediction capabilities. Details of experimental setup, parametric effects on dryout and assessment of correlations can be found in following sections.

Experimental Setup

Experimental setup consists of a closed loop system shown in figure 1, test section was heated by Joule's effect using DC power supply and a water cooled plate type heat exchanger was used to condense the vaporized refrigerant. Stainless steel tube (1.6 mm inside diameter and 245 mm heated length) was used a test section, thermocouples were attached on the outer wall to record the wall temperature while insertion type thermocouples were used to record the bulk fluid temperature (at the inlet and outlet of test section). Gear pump was used to circulate the fluid, System pressure was recorded by an absolute pressure sensor while pressure drop along the test section was recorded by a differential pressure sensor. To electrically isolate the test section from other parts, similar sized glass tubes were used before the inlet and after the outlet of the test section. A 2 μm filter was placed before the inlet of test section to prevent entry of any small particles. Mass flow rate was recorded by a Coriolis mass flow meter. Data logger was connected with computer and HP Agilent VEE was used for data acquisition purpose.

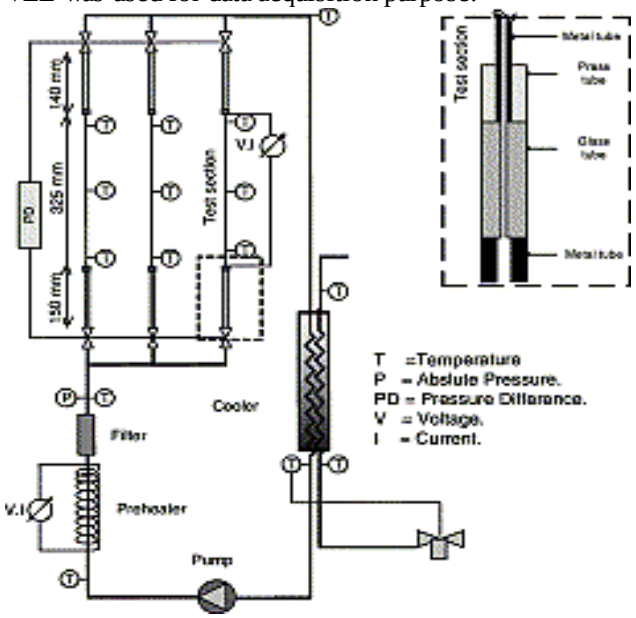

Figure 1 Schematic diagram of the experimental setup

Sufficient time was given after adjusting the system pressure and mass flow rate to achieve the steady state conditions, heat flux was then applied in small increments. After dryout incipience conditions heat flux was increased in very small steps (about 1 kW/m^2) till the completion of dryout. About 100 data-points were recorded for each applied heat flux and their mean value was then used in the calculation. REFPROP 9 was used to get the refrigerant property data.

Roughness for the inner surface of the test section was checked with stylus methodology, figure 2 shows the roughness profile while table 1 summarizes the main parameters for this. R_a represents the arithmetic mean value for the roughness whereas maximum peak height and valley depth is defined by R_p and R_v respectively.

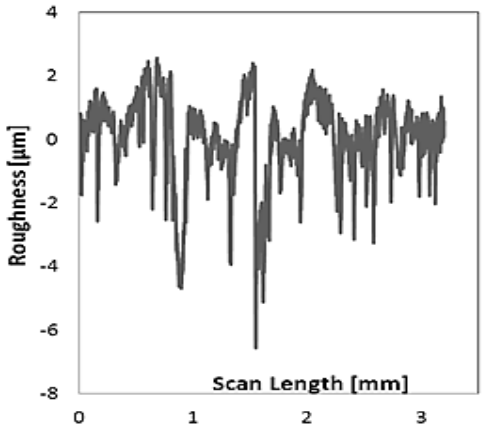

Figure 2 Roughness profile for the heating surface

Table 1 Roughness values

R_a [μm]	R_p [μm]	R_v [μm]
0.95	2.69	6.44

Data reduction

Heat flux applied to the test section was calculated by,

$$\ddot{q} = \frac{V.I}{A_h} \quad (1)$$

Where I and V are the applied current and voltage respectively.A_h is the heated area, $A = \pi d_i l$
Inner wall temperature was calculated from the outer wall temperature by using the solution of steady state one dimensional heat conduction equation (with heat generation) for cylinders, given by,

$$t_{wall\ in} = t_{wall\ out} + \frac{Q}{4\pi kl}\left[\frac{\xi(1-ln\xi)-1}{\xi-1}\right] \quad (2)$$

Where $\xi = \frac{{d_{out}}^2}{{d_{in}}^2}$ and Q is the applied heat power.

Bulk temperature at any axial location (under subcooled conditions) was calculated with the information of bulk inlet temperature and supplied heat as,

$$t_{wall\ in} = t_{wall\ out} + \frac{Q}{4\pi kl}\left[\frac{\xi(1-ln\xi)-1}{\xi-1}\right] \quad (3)$$

Local heat transfer coefficient at any location was calculated by,

$$h_z = \frac{\ddot{q}}{t_{wall\,in} - t_{sat}} \quad (4)$$

Quality/vapor fraction at any axial location is calculated by,

$$x_{th} = \frac{\ddot{q}\pi d_i (z - z_o)}{A_C G h_{fg}} \quad (5)$$

Where z-z_o is the boiling length and h_{fg} is the latent heat of vaporization.

$$z_o = \frac{\dot{m} C_p (t_{sat} - t_{in})}{\ddot{q}\pi d_{in}} \quad (6)$$

Results and Discussion

Boiling curves for 500 kg/m^{2}s are shown in figure 3; this diagram shows variation of heat flux against wall superheat.

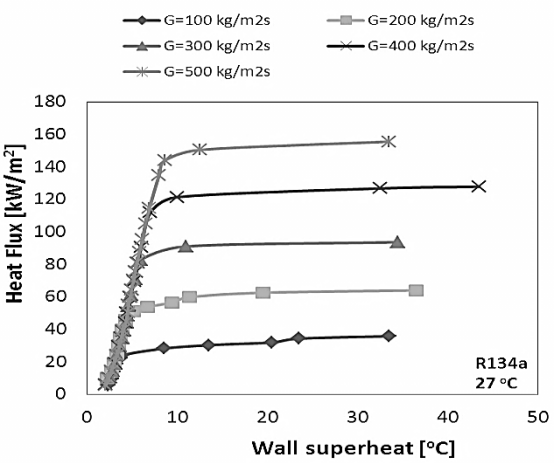

Figure 3 Boiling curve with 500 kg/m^{2}s and at 27 and 32 ^{o}C saturation temperature

Two distinct regions are clear in this boiling curve, initially there is a sharp increase in heat flux with a slight increase in the wall superheat and this follows with the reverse trend in the end. All the diagrams show a sharp increase of wall superheat with a slight change of applied heat flux in the end (right side of each plot) which clearly shows dryout conditions. For the purpose of this study dryout completion was defined by wall superheat > 20 ^{o}C , furthermore electrical relay switched off the power supply when wall temperature approached 70 ^{o}C to save the test section for next test run.

Variation of local wall temperature and heat transfer coefficients for critical heat flux conditions are shown in figure 4. Significant increase in wall temperature and drastic reduction in local heat transfer coefficients close to the outlet of test section are clearly visible.

Dryout incipience and completion heat flux are plotted against vapor quality in figure 5, this diagram shows results for all five mass fluxes at two saturation temperatures. For each mass flux two points are connected with a line, dryout incipience refers to point where boiling curves changes the trend and is at low vapor quality whereas dryout completion refers to the case when no more liquid droplets are there on the wall and wall superheat sharply increases.

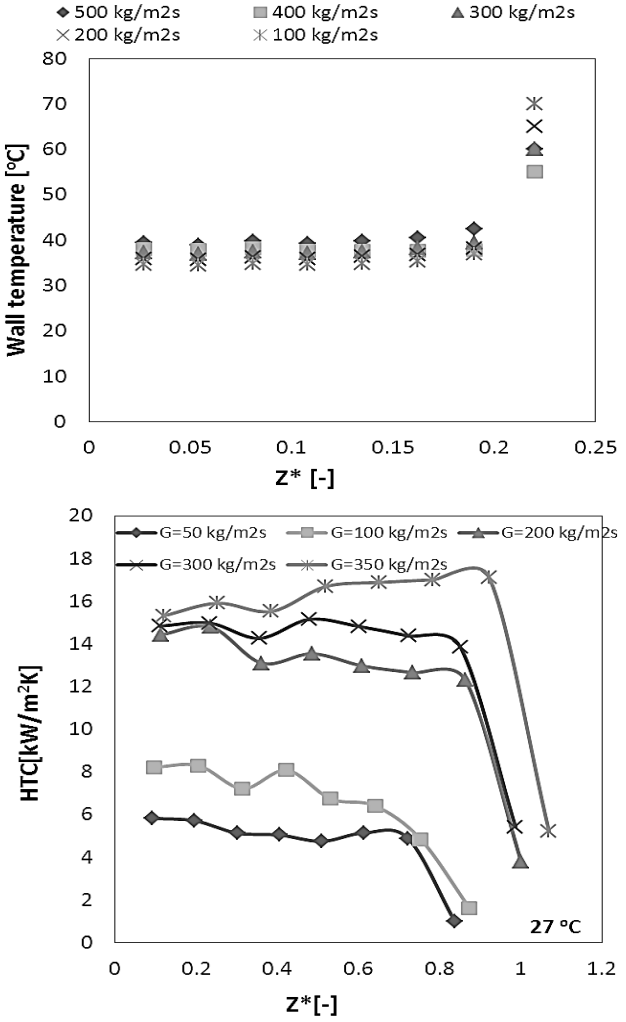

Figure 4 Variation of local wall temperature and local heat transfer coefficients on critical heat flux condition

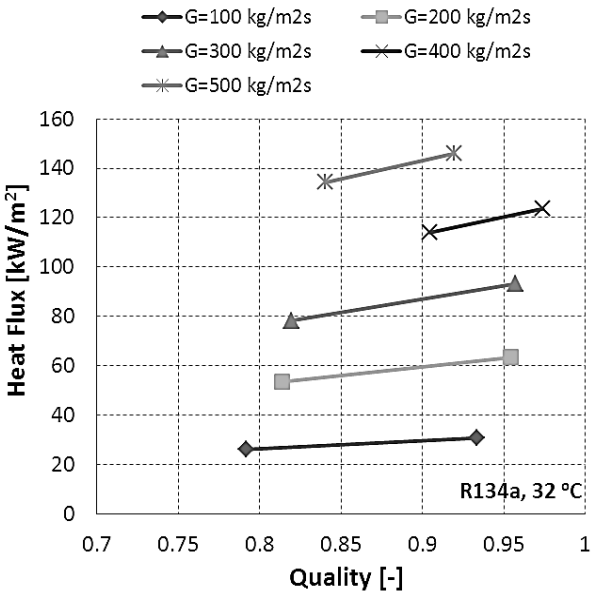

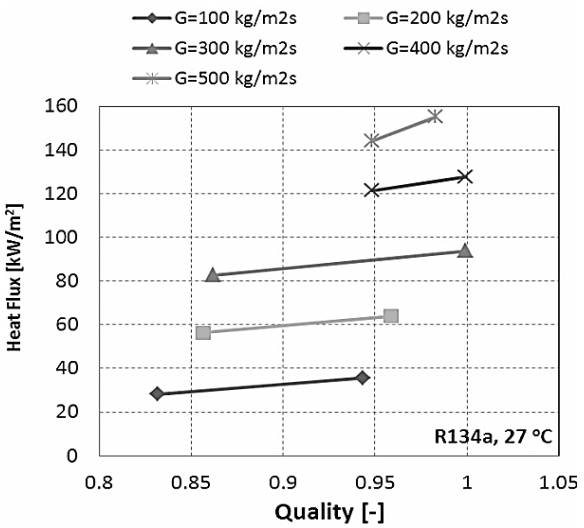

Figure 5 dryout incipience and completion at two saturation temperature for all five mass fluxes

Effect of mass flux, system pressure and vapor quality is shown in figure set 6. Dryout heat flux increases with increasing mass flux as more energy is required to fully vaporize the refrigerant. Dryout heat flux was not affected by variation in system pressure. Vapor quality initially increases with increasing mass flux reaches to a peak at about 400 kg-m2s and then decreases again.

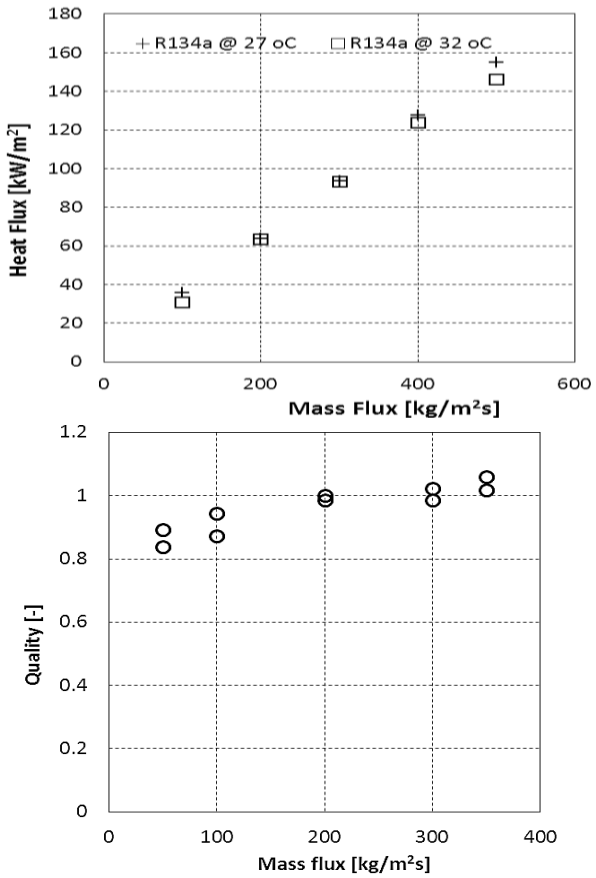

Figure 6 Critical heat flux variation with mass flux, system pressure and vapor quality.

Similar parametric effects were reported by many authors like Maqbool (M. H. Maqbool et al, 2012) for propane in 1.70 mm vertical tube, Ali with R134a in 1.7 mm tube (R. Ali et al, 2011).

Assessment of correlations

This section describes comparison of experimental data with correlations from literature; data was compared by considering mean bias error [MBE] and % age of data within ± 25% from experimental observations. MBE gives information about variance of predicted values from experimental ones and is calculated by $MBE = \frac{1}{N}\sum \frac{h_{predicted} - h_{Experimental}}{h_{Experimental}} * 100$

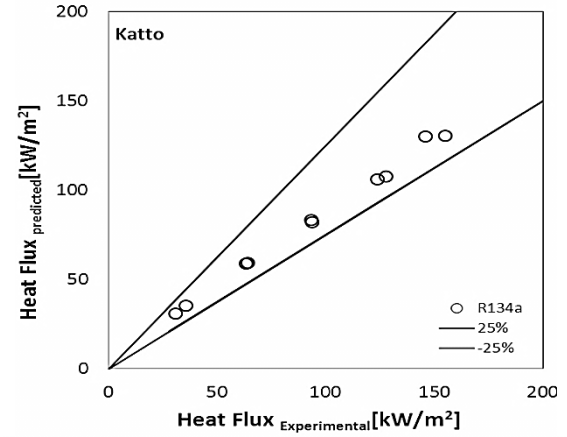

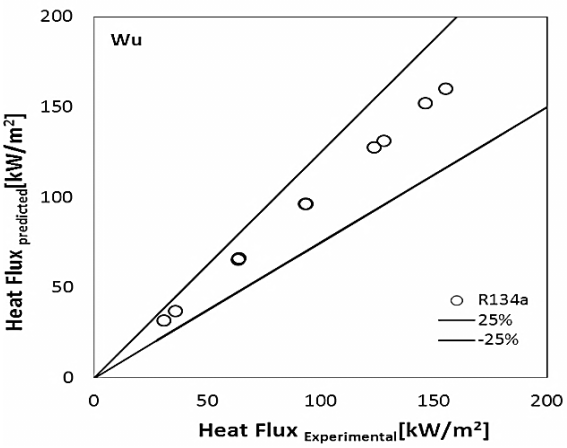

Figure 7 Comparison with Wu and Katto-Ohno correlations

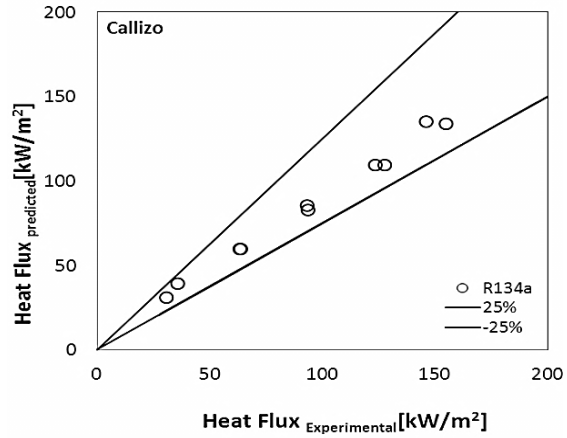

Table 2 Mathematical details for the correlations

Correlation	**Mathematical formulation**	**MBE/% of data**	**Applicability range**
Wu (Z. Wu et al, 2011)	$\frac{\ddot{q}_{CHF}}{Gh_{lg}} = 0.60 * \left(\frac{L_h}{d_{he}}\right)^{-1.19} * {x_{exit}}^{0.817}$ Where $d_{he} = \frac{4A_c}{P_h}$ and P_h is inner perimeter	3.52/100	Saturated flow boiling critical heat flux for microchannels (experimental database had refrigerants, water and nitrogen)
Mikielewicz (D. Mikielewicz et al, 2013)	$\frac{\ddot{q}_{CHF}}{h_{lg}G} = 0.62 \left(\frac{\rho_l}{\rho_g}\right)^{-0.02} (We_D)^{-0.05} \left(\frac{L}{D}\right)^{-1.17}$	9.32/100	Developed from database of SES 36, R134a, R123 & Ethanol in 1.15 and 2.3 mm silver circular channels
Katto&Ohno (Y. Katto et al, 1984)	$\frac{\ddot{q}}{Gh_{lg}} = f\left[\frac{\rho_g}{\rho_l}, \frac{\sigma\rho_l}{G^2L}, \frac{L}{D}\right]$ $with\ no\ subcooling$ $\ddot{q}_{CHF} = \ddot{q}\left[1 + K\frac{h_{in}}{h_{lg}}\right]$	9.58/100	Developed from a large database including water, nitrogen, helium, R12, R22 and R113 in large tubes
Bowring (R. W. Bowring et al, 1972)	$\ddot{q}_{CHF} = \frac{B + 0.25DG\,h_{in}}{C + L}$ $B = \frac{0.5792h_{lg}DGF_1}{1 + 0.0143F_2D^{0.5}G}$ $C = \frac{0.077F_3DG}{1 + 0.347F_4\left(\frac{G}{1356}\right)^n}$ $\dot{p} = \frac{p}{69}$ $F_1 = \frac{\left[\dot{p}^{18.942}exp\left(20.8(1-\dot{p})\right) + 0.917\right]}{1.917}$ $\frac{F_1}{F_2} = \frac{\left[\dot{p}^{1.316}exp\left(2.444(1-\dot{p})\right) + 0.309\right]}{1.309}$ $F_3 = \frac{\left[\dot{p}^{17.023}exp\left(16.658(1-\dot{p})\right) + 0.667\right]}{1.667}$ $\frac{F_4}{F_3} = \dot{p}^{1.649}$ $n = 2 - 0.5\dot{p}$	14.59/90	Developed from a wide database of water in large tubes
Ong (C. L. Ong et al, 2011)	$\frac{\ddot{q}}{Gh_{lg}} = 0.12 \left(\frac{\mu_l}{\mu_g}\right)^{0.183} \left(\frac{\rho_v}{\rho_l}\right)^{0.062} {We_L}^{-0.141} \left(\frac{L_{ev}}{D}\right)^{-0.7} \left(\frac{D}{D_{th}}\right)^{0.11}$ Where $D_{th} = \frac{1}{Co}\sqrt{\frac{\sigma}{g(\rho_l - \rho_g)}}$	15.96/100	Revised version of Wojtan's correlation Developed from a database including R134a, R245fa, R236fa and data from single and mulitchannels
Callizo (C. M. Callizo et al, 2010)	$\frac{\ddot{q}_{CHF}}{h_{lg}G} = 0.3216 \left(\frac{\rho_g}{\rho_l}\right)^{0.084} (We_L)^{-0.034} \left(\frac{L}{D}\right)^{-0.942}$	8.96/100	Modified form of Wojtan's correlation based on experiments with R134a, R245fa & R22 in a vertical circular 640 μm test section
Wojtan (L. Wojtan et al, 2006)	$\frac{\ddot{q}_{CHF}}{h_{lg}G} = 0.437 \left(\frac{\rho_g}{\rho_l}\right)^{0.073} (We_L)^{-0.24} \left(\frac{L}{D}\right)^{0.72}$	9.59/100	Revised version of Katto-Ohno correlation Least square curve fitting for R134a and R245fa in 0.5 and 0.8 mm circular channels
Qi (S. L. Qi et al, 2007)	$\frac{\ddot{q}_{CHF}}{h_{lg}G} = (0.214 + 0.140 * C_o)\left(\frac{\rho_g}{\rho_l}\right)^{0.133} (We_L)^{-0.333}$	14.85/90	Revised version of Katto-Ohno correlation based on boiling of nitrogen in small tubes (0.531-1.931 mm)

Bowers and Mudawar (M. B.Bowers et al, 1994)	$\frac{\ddot{q}}{Gh_{lg}} = 0.16\, We^{-0.19}\left(\frac{L}{D}\right)^{-0.54}\left(\frac{1}{1+0.03\,{}^{L}/_{D}}\right)$	43.64/40	Developed from R113 in 0.51 & 2.54 mm multichannel arrangement
Zhang (W. Zhang et al, 2006)	$\frac{\ddot{q}_{CHF}}{h_{lg}G} = 0.0352\left[We_D + 0.0119\left(\frac{L}{D}\right)^{2.31}\left(\frac{\rho_g}{\rho_l}\right)^{0.361}\right]^{-0.295}\left(\frac{L}{D}\right)^{-0.311}\left[2.05\left(\frac{\rho_g}{\rho_l}\right)^{0.170} - x_{in}\right]$	34.45/0	Developed from experimental database on saturated flow boiling of water in small diameter tubes (0.33-6.2 mm)

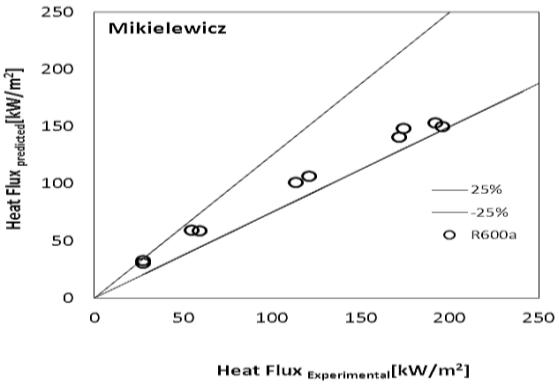

Figure 8 Comparison with Mikielewicz and Callizo correlations

Mathematical formulation for the correlations and summary of comparison can be found in table 2.

Experimental data was compared with most quoted Katto-Ohno (Y. Katto et al, 1984) correlation, this was originally developed for conventional sized channels (d_h>3 mm) however many authors found good prediction when applied to mini/micro channels. Comparison of our experimental data shows good predictions with correlation.

Callizo (C. M. Callizo et al, 2010) proposed modified version of Katto-Ohno (Y. Katto et al, 1984) correlation based on their data base. All the data points were accurately predicted within the 25% span by using this correlation.

Wu (Z. Wu et al, 2011) and Mikielewicz (D. Mikielewicz et al, 2013) proposed empirical correlation based on their experimental data bases (minichannel with various fluids). Comparison of our data showed good prediction with these correlations.

Conclusions

Experimental findings on dryout of R 134a in a vertical minichannel were reported in this study. Results are briefly summarized here,

- Dryout heat flux increased with increasing mass flux however no effect of varying system pressure was observed.
- Critical mass quality initially increased with increasing mass flux reached to a peak value and then decreased again.
- Among macro scale correlations Katto-Ohno (Y. Katto et al, 1984) correlation accurately predicted the data while from micro side Wu (Z. Wu et al, 2011), Callizo (C. M Callizo et al, 2010) &Mikielewicz (D. Mikielewics et al, 2013) predicted the data.

Nomenclature

A_c Cross sectional area [m^2]

B,C,F_1-F_4,n, Parameters in Bowring correlation

Co Confinement No [-]

C_p Specific heat capacity [J/kg.K]

d_h Inner diameter of the test section [m]

G Mass Flux [kg/m^2s]

h_{in} Inletenthalpy [kJ/kg]

h_{lg} Enthalpy of vaporization [kJ/kg]

I Current [A]

k Thermal conductivity [w/m^2K]

L_h Effective/heated length [m]

$\dot{m}$ Mass flow rate [kg/sec]

MBE Mean Bias Error

$$MBE = \frac{1}{N}\sum_{1}^{N}\frac{\left|\ddot{q}_{CHF\,predicted} - \ddot{q}_{CHF\,Experimental}\right|}{\ddot{q}_{CHF\,Experimental}}$$

Q Applied electric power [W]

$\ddot{q}$ Heat Flux [W/m^2]

$\ddot{q}_{CHF}$ Critical heat flux [W/m^2]

t_{sat} Saturation temperature [^oC]

V Voltage [V]

We Webber No [-]

x Vapor quality [-]

z Axial position [m]

Greek letters

μ viscosity [Pa-s]

ρ Density [kg/m^3]

σ Surface Tension [N/m]

Subscript

CHF Critical heat flux

g gas phase

l liquid phase

References

S. Kandlikar,(2006) Heat transfer and fluid flow in minichannels and microchannels, *Elsevier*.

C. L. Ong and J. R. Thome, (2011) Macro-to-microchannel transition in two-phase flow: Part 2 – Flow boiling heat transfer and critical heat flux, *Experimental thermal and fluid science*, vol. 35, pp. 873-886.

L. Wojtan, R. Revellin and J. R. Thome, (2006) Investigation of saturated critical heat flux in a single, Uniformly heated microchannel, *Experimental thermal and fluid science*, pp. 765-774.

D. Mikielewicz, J. Wajs, M. Glinski, (2013) A. Baset and R. S. Zrooga, Experimental investigation of dryout of SES 36, R134a, R123 and ethanol in vertical small diameter tubes, *Experimental thermal and fluid science*, pp. 556-564.

C. M. Callizo, (2010) Flow boiling heat transfer in single vertical channels of small diameters, *KTH*, Stockholm.

R. Ali and B. Palm, (2011) Dryoutcharacteristics during flow boiling of R134a in vertical circular minichannels, vol. 54, no.

M. H. Maqbool, B. Palm and R. Khodabandeh, (2012) Experimental investigation of dryout of propane in uniformly heated single vertical mini-channels, *Experimental thermal and fluid science*, pp. 121-129.

Y. Katto and H. Ohno, (1984) An improved version of the generalized correlation for critical heat flux for forced convective boiling in uniformly heated vertical tubes, *International Journal of Heat and Mass transfer*, pp. 1641-1648.

R. W. Bowring, (1972) A simple but accurate round tube uniform heat flux correlation over the pressure range 0.7-17 MN/m2, Winfrith.

Z. Wu, W. Li and S. Ye, (2011) Correlations for saturated critical heat flux in microchannels, *International Journal of Heat and Mass transfer*, pp. 379-389.

S. L. Qi, P. Zhang, R. Z. Wang and L. X. Xu, (2007) Flow boiling of liquid nitrogen in micro-tubes: Part II – Heat transfer characteristics and critical heat flux, *International Journal of Heat and Mass transfer* , pp. 5017-5030.

M. B. Bowers and I. Mudawar, (1994) High flux boiling in low flow rate, low pressure drop mini-channel and micro-channel heat sinks, *International Journal of Heat and Mass transfer*, pp. 321-332.

W. Zhang, T. Hibiki, K. Mishima and Y. Mi, (2006) Correlation of critical heat flux for flow boiling of water in mini-channels, *International Journal of heat and mass transfer* , pp. 1058-1072.